Macromolecules

Article

pubs.acs.org/Macromolecules

Alternating Copolymers Incorporating Dithienogemolodithiophene for Field-Effect Transistor Applications

Jessica Shaw,[†] Hongliang Zhong,[†] Chin Pang Yau,[†] Abby Casey,[†] Ester Buchaca-Domingo,[‡] Natalie Stingelin,[‡] David Sparrowe,[§] William Mitchell,[§] and Martin Heeney*,[†]

[†]Department of Chemistry and Centre for Plastic Electronics and [‡]Department of Materials and Centre for Plastic Electronics, Imperial College London, Exhibition Road, South Kensington, London SW7 2AZ, United Kingdom

[§]Merck Chemicals Ltd., Chilworth Technical Centre, University Parkway, Southampton SO16 7QD, United Kingdom

Supporting Information

ABSTRACT: We report the synthesis of an electron-rich fused dithienogemolodithiophene monomer containing straight chain tetradecyl solubilizing groups. Copolymers were prepared with four different electron accepting monomers of varying reduction potential. We report how the choice of acceptor influences the optical properties and molecular energy levels as well as the solid state packing. Field effect transistor devices were fabricated using silver source-drain electrodes, with a promising charge carrier mobility up to 0.26 $cm^2\ V^{-1}\ s^{-1}$ for films deposited from non-chlorinated solvents. These results suggest dithienogemolodithiophene is a useful building block for the development of high performance semiconducting polymers.

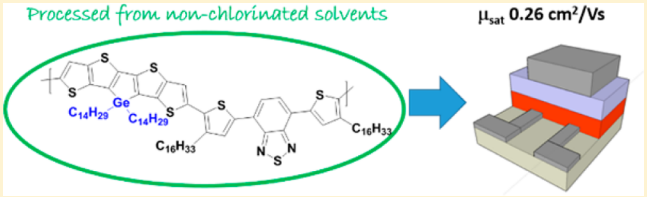

INTRODUCTION

The potential of fully printable electronics as a low-cost, lightweight alternative to traditional silicon-based electronics has resulted in a significant amount of interest in recent years in the development of solution processable, organic semiconductors.[1−6] There has been tremendous progress in this area over the past decade, with the field effect mobility of semiconducting polymers improving several orders of magnitude, to values commensurate with or even exceeding amorphous silicon, the benchmark large area inorganic semiconductor.[7−23] However, in order to enable the next generation of printable electronics, organic semiconducting materials with even higher charge carrier mobilities and very stable device characteristics are currently sought.

Polymers containing rigid, highly fused multi-ring aromatics are particularly promising for this application.[24−28] The use of rigid building blocks can reduce conformational disorder along the backbone, enhancing polymer planarity and reducing the reorganizational energy associated with charge hopping. However, a common drawback with the use of highly fused building blocks is reduced polymer solubility; therefore, judiciously placed solubilizing groups are required along the backbone as well as the use of comonomers which contain solubilizing groups. The nature of the side chains is known to have an important role in the solid state packing and aggregation of the polymers.[29,30] In general, branched alkyl side chains have the most beneficial impact on polymer solubility and are often utilized in polymers for solar cell applications, where it is important that the polymer crystallinity is moderated to ensure good mixing with the acceptor fullerene material. For transistor applications, where it is important to maximize intermolecular contacts, straight chain alkyl side chains have typically been utilized. More recently, it has been shown that branched side chains can be effective in charge transport polymers if the branching point is moved further away from the conjugated backbone.[31−33]

Recently we reported the synthesis and promising OPV performance of a series of donor−acceptor polymers containing a five-ring fused dithienogemolodithiophene (DTTG) unit, which were solubilized with branched 2-ethylhexy or 2-octyldodecyl side chains.[34,35] The nature of the side chain was shown to have a major impact on the solar cell performance, but the transistor performance was not investigated. The DTTG unit can be thought of as an extended version of dithienogermole (DTG), in which an additional thiophene ring is appended to either side of the monomer. Copolymers of DTG itself have already shown reasonable performance in transistor devices with charge carrier mobilities up to 0.11 $cm^2\ V^{-1}\ s^{-1}$ reported for copolymers with 2,1,3-benzothiadiazole (BT),[36] suggesting that extended analogues may be of interest. Moreover, Xu and co-workers have shown that the charge carrier mobility of indacenodithiophene (IDT)-based copolymers can be significantly improved by extending the ring system with an additional thiophene.[24] Hence, substitution of the terminal thiophenes in IDT with thieno[3,2-*b*]thiophene formed the fully conjugated, seven-membered, ring fused, indacenodithieno[3,2-*b*]thiophene (IDTT) unit. The inclusion of the IDTT unit extended the effective

Received: October 14, 2014
Revised: November 25, 2014
Published: December 11, 2014

   dx.doi.org/10.1021/ma5021038 | *Macromolecules* 2014, 47, 8602−8610

conjugation of the polymer backbone, resulting in the observed increase in charge carrier mobility. Hence, in this study we aimed to investigate the potential of DTTG containing polymers with straight chain solubilizing groups for use as transistor materials.

EXPERIMENTAL SECTION

All starting materials and reagents were purchased from commercial sources (Sigma-Aldrich, VWR, and Wawei Chemicals Ltd.) and used as received, unless otherwise stated. All reactions were conducted under argon using standard Schlenk line techniques using anhydrous solvents as commercially supplied. The ^{1}H and ^{13}C NMR spectra for chemical intermediates were recorded on a Bruker AV-400 (400 MHz) spectrometer at 298 K in either chloroform-*d* or acetone-d_6. The ^{1}H NMR spectra for polymers were recorded on a Bruker AV-500 (500 MHz) spectrometer at 403 K in d_2-1,1,2,2-tetrachloroethane. Chemical shifts are reported in ppm relative to residual protons in the deuterated solvent used. MestReNova v7.1.2 from MestreLab was used to analyze all spectra. Electrospray ionization (ESI) mass spectrometry was performed with a Micromass LCT Premier Instrument. Elemental analysis was performed with a Thermo Flash 2000 machine. Flash column chromatography was performed using silica gel (Merck Kieselgel 60 grade 40−63 μm F254). Thin layer chromatography (TLC) was performed on Merck Kieselgel 60 F254 aluminum sheets and observed under 254 nm UV light. All microwave experiments were performed in a Biotage Initiator v2.3. Final stannylated monomers were purified using a Shimadzu preparative gel permeation chromatograph (GPC) in hexane at 40 °C. Polymers were purified using a Shimadzu preparative GPC in chlorobenzene at 80 °C. The system consists of a DGU-20A3 degasser, an LC-20A pump, a CTO-20A column oven, an Agilent PLgel 10 μm MIXED-D column, and a SPD-20A UV detector. Number-average (M_n) and weight-average (M_w) molecular weights were determined with an Agilent Technologies 1200 series GPC in chlorobenzene at 80 °C, using two PL mixed B columns in series. The machine was calibrated against narrow weight polydispersity polystyrene standards. Solution and solid-state UV−vis absorption spectra were recorded on a UV-1800 Shimadzu UV−vis spectrometer. Polymer thin films were spin-cast on glass substrates from chlorobenzene solutions (5 mg/mL) using a Laurell WS-400BZ-6NPP/LITE spin-coater. Photoelectron spectroscopy in air (PESA) measurements were recorded with a Riken Keiki AC-2 PESA spectrometer with a power setting of 5 nW and a power number of 0.5. Differential scanning calorimetry (DSC) experiments were carried out with a TA Instruments DSC TZero Q20 v24.10 instrument at a scan rate of 10 °C/min and analyzed using TA Instruments Universal Analysis 2000 v4.5A software. Thermal gravimetric analysis (TGA) plots were obtained with a PerkinElmer Pyris 1 TGA. X-ray diffraction (XRD) measurements were performed on a Panalytical X'Pert-pro MRD diffractometer equipped with a nickel-filtered Cu Kα_1 beam and X'Celerator detector using a 40 mA current and 40 kV accelerating voltage. Polymer thin films were drop-cast on glass substrates from 1,2-dichlorobenzene solutions (7 mg/mL) and annealed for 2 min at 100, 150, or 175 °C under argon. Density functional theory (DFT) calculations were carried out using the Gaussian 03[37] and 09[38] programs with the Becke three-parameter, Lee−Yang−Parr, (B3LYP) hybrid functional level of theory and a basis set of 6-311G(D).

(3,3′-Dibromo-2,2′-bithieno[3,2-*b*]thiene-5,5′-diyl)bis-(trimethylsilane) (**1**),[35] diphenylbis(tetradecyl)germane (**2a**),[36] dibromobis(tetradecyl)germane (**2**),[36] 1,3-dibromo-5-octyl-4*H*-thieno-[3,4-*c*]pyrrole-4,6(5*H*)-dione (TPD),[39] *N*,*N*′-bis(*n*-octyl)-2,6-dibromonaphthalene-1,4,5,8-tetracarboxylic diimide (NDI),[40] 4,7-bis(5-bromo-4-hexadecylthiophen-2-yl)-benzo[1,2,5-*c*]thiadiazole (DTBT-C_{16}),[41] and 4,7-bis(5-bromothiophen-2-yl)-5,6-bis(octyloxy)benzo-[1,2,5-*c*]thiadiazole (DTBT-OC_8)[42] were synthesized using previously reported procedures.

Top gate, bottom contact OFETs were fabricated on glass substrates with photolithographically defined silver source-drain electrodes. Polymer films were spin-cast on top from 1,2-dichlorobenzene solutions (7 mg/mL) and annealed at 100 and 150 °C for 2 min before a fluoropolymer dielectric (Lisicon D139, Merck, Germany) was spin-cast on top. All fabrication and annealing were performed in an ambient atmosphere. In selected cases, polymer films were spin-cast from 1,3,5-trimethylbenzene:1-methylnaphthalene solutions (7 mg/mL) and annealed at 150 °C for 2 min. Finally, a photolithographically defined silver gate electrode was deposited. Electrical characterization was carried out in ambient atmosphere using an Agilent 4155C semiconductor parameter analyzer.

Diphenylbis(tetradecyl)germane (2a). Tetradecylmagnesium chloride solution (15.4 mL of a 1.0 M solution in THF, 15.4 mmol) was added dropwise to a stirred solution of diphenylgermanium dichloride (1.5 g, 5.1 mmol) in anhydrous tetrahydrofuran (25 mL) at 0 °C under an argon atmosphere. Once the addition was complete, the reaction mixture was warmed to room temperature, stirred for 30 min, and then refluxed for 16 h. The reaction mixture was cooled to 0 °C and quenched with methanol (10 mL). The resulting solution was diluted with ethyl acetate (20 mL) and washed with water (3 × 15 mL) and brine (15 mL). After drying ($MgSO_4$), the volatiles were removed *in vacuo*. Purification of the crude product by column chromatography over silica (eluent: hexane) gave the title compound (2.1 g, 3.3 mmol, 65%) as a colorless oil. ^{1}H NMR (400 MHz, acetone-d_6): 7.47 (m, 4H, Ar*H*), 7.35 (m, 6H, Ar*H*), 1.47 (m, 4H, −CH_2−), 1.27 (m, 48H, −CH_2−), 0.87 (t, 6H, −CH_3). ^{13}C NMR (100 MHz, acetone-d_6): 139.83, 135.37, 129.58, 129.13, 34.29, 32.93, 30.73−30.60 (overlapping C), 30.53, 30.38, 30.14, 25.97, 23.62, 14.66, 13.95. Anal. Calcd for ($C_{40}H_{68}Ge$): C, 77.29; H, 11.03. Found: C, 77.13; H, 11.14.

Dibromobis(tetradecyl)germane (2b). Bromine (0.43 mL, 8.4 mmol) in anhydrous 1,2-dichloroethane (5 mL) was added dropwise to a solution of diphenylbis(tetradecyl)germane (2.5 g, 4.0 mmol) in anhydrous 1,2-dichloroethane (50 mL) in the absence of light. The reaction mixture was heated to reflux for 5 h and then cooled to room temperature. The resulting solution was concentrated under vacuum and then dried under high vacuum to give the title compound (2.4 g, 3.8 mmol, 95%) as a pale orange oil. ^{1}H NMR (400 MHz, $CDCl_3$): 1.74 (m, 4H, −CH_2−), 1.62 (m, 4H, −CH_2−), 1.40 (m, 4H, −CH_2−), 1.26 (s, 40H, −CH_2−), 0.88 (t, 6H, −CH_3). ^{13}C NMR (100 MHz, $CDCl_3$): 32.09, 31.77, 29.83−29.76 (overlapping C), 29.57, 29.52, 29.20, 28.23, 24.41, 22.85, 14.28. Anal. Calcd for ($C_{28}H_{58}Br_2Ge$): C, 53.62; H, 9.32. Found: C, 53.50; H, 9.39.

[9,9-Bis(tetradecyl)-9*H*-thieno[3,2-*b*]thieno[2″,3″:4′,5′]-thieno[2′,3′:4,5]germolo[2,3-*d*]thiene-2,7-diyl]bis-(trimethylsilane) (3). *n*-Butyllithium (4.3 mL of a 1.6 M solution in hexanes, 6.9 mmol) was added dropwise to a stirred solution of 3,3′-dibromo-2,2′-bithieno[3,2-*b*]thiene-5,5′-diylbis(trimethylsilane) (**1**) (2.0 g, 3.5 mmol) in anhydrous diethyl ether (200 mL) at −90 °C under an argon atmosphere. The reaction mixture was stirred for 30 min before a solution of dibromobis(tetradecyl)germane (**2**) (2.3 g, 3.6 mmol) in anhydrous diethyl ether (5 mL) was added dropwise. Once the addition was complete, the reaction mixture was allowed to warm to room temperature overnight and quenched with wet diethyl ether. The mixture was further diluted with diethyl ether (50 mL), washed with water (3 × 50 mL) and brine (50 mL), and dried ($MgSO_4$) and the volatiles removed *in vacuo*. Purification by column chromatography over silica (eluent: hexane) yielded the title compound (1.7 g, 1.9 mmol, 54%) as yellow oil. ^{1}H NMR (400 MHz, acetone-d_6): 7.52 (s, 2H, Ar*H*), 1.60 (m, 4H, −CH_2−), 1.43 (m, 4H, −CH_2−), 1.33 (m, 4H, −CH_2−), 1.26 (s, 40H, −CH_2−), 0.87 (t, 6H, −CH_3), 0.37 (s, 18H, −CH_3). ^{13}C NMR (100 MHz, acetone-d_6): 150.25, 148.71, 143.33, 134.07, 127.24, 33.32, 32.67, 30.49−30.42 (overlapping C), 30.40, 30.23, 30.17, 29.98, 26.40, 23.37, 14.97, 14.41. ESI (*m*/*z*) 889 ([M + H]$^+$, 4%). Calcd: 889.3815. Found: 889.3808.

2,7-Dibromo-9,9-bis(tetradecyl)-9*H*-thieno[3,2-*b*]thieno-[2″,3″:4′,5′]thieno[2′,3′:4,5]germolo[2,3-*d*]thiophene (4). *N*-Bromosuccinimide (251 mg, 1.4 mmol) was added in several portions to a stirred solution of [9,9-bis(tetradecyl)-9*H*-thieno[3,2-*b*]thieno-[2″,3″:4′,5′]thieno[2′,3′:4,5]germolo[2,3-*d*]thiene-2,7-diyl]bis-(trimethylsilane) (**3**) (620 mg, 0.7 mmol) in anhydrous tetrahydrofuran (60 mL) in the absence of light. Once the addition was complete, the reaction was stirred overnight. An aqueous solution of

dx.doi.org/10.1021/ma5021038 | *Macromolecules* 2014, 47, 8602−8610

sodium sulfite (20 mL) was then added, and the crude product was extracted with diethyl ether (25 mL). The organics were washed with water (3 × 25 mL), brine (25 mL), and dried ($MgSO_4$), and the volatiles removed *in vacuo*. Purification of the crude product by column chromatography over silica (eluent: hexane) gave the title compound as a yellow oil (410 mg, 0.5 mmol, 65%). ^{1}H NMR (400 MHz, acetone-d_6): 7.58 (s, 2H, Ar*H*), 1.56 (m, 4H, $-CH_2-$), 1.47 (m, 4H, $-CH_2-$), 1.23 (s, 44H, $-CH_2-$), 0.87 (t, 6H, $-CH_3$). ^{13}C NMR (100 MHz, $CDCl_3$): 147.83, 143.34, 138.85, 133.44, 122.69, 111.75, 32.93, 32.10, 29.87−29.84 (overlapping C), 29.75, 29.61, 29.54, 29.26, 25.77, 22.87, 14.49, 14.30. Anal. Calcd for ($C_{40}H_{60}Br_2GeS_4$): C, 53.29; H, 6.71. Found: C, 53.37; H, 6.80.

2,7-Bis(trimethylstannyl)-9,9-bis(tetradecyl)-9*H*-thieno[3,2-*b*]thieno[2″,3″:4′,5′]thieno[2′,3′:4,5]germolo[2,3-*d*]thiophene (5). *tert*-Butyllithium (3.4 mL of a 1.7 M solution in pentane, 5.7 mmol) was added dropwise to a stirred solution of 2,7-dibromo-9,9-bis(tetradecyl)-9*H*-thieno[3,2-*b*]thieno[2″,3″:4′,5′]thieno[2′,3′:4,5]-germolo[2,3-*d*]thiophene (**4**) (1.1 g, 1.3 mmol) in anhydrous diethyl ether (300 mL) at −90 °C under an argon atmosphere. The reaction mixture was stirred for 30 min at this temperature before a solution of trimethyltin chloride (6.1 mL of a 1.0 M solution in THF, 6.1 mmol) was added dropwise. Once the addition was complete, the reaction mixture was allowed to warm to room temperature overnight. An aqueous solution of sodium bicarbonate (25 mL) was then added, and the crude product was extracted with diethyl ether (50 mL). The organics were then washed with water (3 × 50 mL) and brine (50 mL) and dried (Na_2SO_4), and the volatiles were removed *in vacuo*. Purification of the crude product by recycling GPC (hexane) gave the title compound as a yellow oil (948 mg, 0.9 mmol, 70%). ^{1}H NMR (400 MHz, acetone-d_6): 7.45 (s, 2H, Ar*H*), 1.61 (m, 4H, $-CH_2-$), 1.42 (m, 4H, $-CH_2-$), 1.27 (s, 44H, $-CH_2-$), 0.87 (t, 6H, $-CH_3$), 0.42 (s, 18H, $-CH_3$). ^{13}C NMR (100 MHz, acetone-d_6): 149.50, 149.33, 143.44, 141.83, 133.67, 128.12, 33.40, 32.77, 30.52−29.37 (overlapping C) 26.50, 23.46, 15.04, 14.50, −8.07.

Poly-2,7(9,9-bis(tetradecyl)-9*H*-thieno[3,2-*b*]thieno-[2″,3″:4′,5′]thieno[2′3′:4,5]germolo[2,3-*d*]thiophene)-*alt*-1,3(5-octyl-4*H*-thieno[3,4-*c*]pyrrole-4,6(5*H*)-dione) (pDTTG-TPD). An oven-dried microwave vial equipped with a stir bar was charged with 2,7-bis(trimethylstannyl)-9,9-bis(tetradecyl)-9*H*-thieno-[3,2-*b*]thieno[2″,3″:4′,5′]thieno[2′,3′:4,5]germolo[2,3-*d*]thiophene (**5**) (219.8 mg, 0.2055 mmol), 1,3-dibromo-5-octyl-4*H*-thieno[3,4-*c*]pyrrole-4,6(5*H*)-dione (87.0 mg, 0.2055 mmol), tris-(dibenzylideneacetone)dipalladium(0) (3.8 mg, 0.0041 mmol), and tri(*o*-tolyl)phosphine (5.0 mg, 0.0164 mmol). The vial was purged with argon before anhydrous chlorobenzene (0.5 mL) was added. The reaction mixture was purged with argon for a further 30 min and then subjected to the following microwave conditions: 100 °C for 2 min, 120 °C for 2 min, 140 °C for 2 min, 160 °C for 2 min, 180 °C for 20 min, and 200 °C for 20 min. Once the reaction mixture had cooled, the crude product was precipitated in methanol, filtered through a Soxhlet thimble, and purified by Soxhlet extraction with methanol (24 h), acetone (24 h), and hexane (24 h). The polymer was extracted into hexane, and the resulting solution was concentrated under reduced pressure. The residue was dissolved in chloroform and vigorously stirred with an aqueous sodium diethyldithiocarbamate solution (ca. 0.5 g in 100 mL) at 50 °C for 2 h. After cooling, the organics were extracted with chloroform (50 mL), combined, and washed with water (3 × 50 mL). The solution was concentrated under vacuum and precipitated in methanol. The resulting precipitate was isolated by filtration to yield the title compound as a dark purple solid (157.6 mg, 76%). M_n = 7 kDa, M_w = 10 kDa, $Đ$ = 1.5. ^{1}H NMR (500 MHz, d_2-1,1,2,2-tetrachloroethane): 8.45 (br, 2H, Ar*H*), 3.72 (br, 2H, $-NCH_2-$), 1.32 (br, 64H, $-CH_2-$), 0.93 (br, 9H, $-CH_3$). Anal. Calcd for ($C_{54}H_{77}GeNO_2S_5$)$_n$: C, 64.53; H, 7.72; N, 1.39. Found: C, 64.42; H, 7.81; N, 1.44.

Poly-2,7(9,9-bis(tetradecyl)-9*H*-thieno[3,2-*b*]thieno-[2″,3″:4′,5′]thieno[2′3′:4,5]germolo[2,3-*d*]thiophene)-*alt*-4,7-bis(5-thiophen-2-yl)-5,6-bis(octyloxy)benzo[1,2,5-*c*]-thiadiazole (pDTTG-DTBT(OC$_8$)). An oven-dried microwave vial equipped with a stir bar was charged with 2,7-bis(trimethylstannyl)-9,9-bis(tetradecyl)-9*H*-thieno[3,2-*b*]thieno[2″,3″:4′,5′]thieno-[2′,3′:4,5]-germolo[2,3-*d*]thiophene (**5**) (263.4 mg, 0.2463 mmol), 4,7-bis(5-bromothiophen-2-yl)-5,6-bis(octyloxy)benzo[1,2,5-*c*]-thiadiazole (176.0 mg, 0.2463 mmol), tris(dibenzylideneacetone)-dipalladium(0) (4.5 mg, 0.0049 mmol), and tri(*o*-tolyl)phosphine (6.0 mg, 0.0197 mmol). The vial was purged with argon before anhydrous chlorobenzene (0.5 mL) was added. The reaction mixture was purged with argon for a further 30 min and reacted as above. After precipitation into methanol, the polymer was filtered through a Soxhlet thimble and purified by Soxhlet extraction with methanol (24 h), acetone (24 h), hexane (24 h), and chloroform (3 h). The remaining polymer residue was dissolved in 1,1,2,2-tetrachloroethane and heated to 140 °C overnight. After cooling, the solution was filtered hot, concentrated under vacuum, and precipitated in acetone. The resulting precipitate was isolated by filtration to yield the title compound as a dark purple solid (54.9 mg, 17%). M_n = 35 kDa, M_w = 88 kDa, $Đ$ = 2.5. ^{1}H NMR (500 MHz, d_2-1,1,2,2-tetrachloroethane): 8.49 (br, 2H, Ar*H*), 7.45 (br, 4H, Ar*H*), 4.30 (br, 4H, $-CH_2-$), 2.06 (br, 4H, $-CH_2-$), 1.73 (br, 4H, $-CH_2-$), 1.59 (br, 4H, $-CH_2-$), 1.33 (br, 64H, $-CH_2-$), 0.95 (br, 12H, $-CH_3$). Anal. Calcd for ($C_{70}H_{98}GeN_2O_2S_7$)$_n$: C, 64.84; H, 7.62; N, 2.16. Found: C, 64.92; H, 7.54; N, 2.25.

Poly-2,7(9,9-bis(tetradecyl)-9*H*-thieno[3,2-*b*]thieno-[2″,3″:4′,5′]thieno[2′3′:4,5]germolo[2,3-*d*]thiophene)-*alt*-*N*,*N*′-bis(*n*-octyl)-2,6-naphthalene-1,4,5,8-tetracarboxylic Diimide (pDTTG-NDI). An oven-dried microwave vial equipped with a stir bar was charged with 2,7-bis(trimethylstannyl)-9,9-bis(tetradecyl)-9*H*-thieno[3,2-*b*]thieno[2″,3″:4′,5′]thieno[2′,3′:4,5]-germolo[2,3-*d*]-thiophene (**5**) (258.4 mg, 0.2416 mmol), *N*,*N*′-bis(*n*-octyl)-2,6-dibromonaphthalene-1,4,5,8-tetracarboxylic diimide (156.6 mg, 0.2416 mmol), tris(dibenzylideneacetone)dipalladium(0) (4.4 mg, 0.0048 mmol), and tri(*o*-tolyl)phosphine (5.9 mg, 0.0193 mmol). The vial was purged with argon before anhydrous chlorobenzene (0.5 mL) was added. The reaction mixture was purged with argon for a further 30 min and reacted as above. The crude product was precipitated in methanol, filtered through a Soxhlet thimble, and purified by Soxhlet extraction with methanol (24 h), acetone (24 h), hexane (24 h), and chloroform (3 h). The chloroform extract was vigorously stirred with an aqueous sodium diethyldithiocarbamate solution (ca. 0.5 g in 100 mL) at 50 °C for 2 h. After cooling, the organics were extracted with chloroform (50 mL), combined, and washed with water (3 × 50 mL). The solution was concentrated under vacuum and precipitated in methanol. The resulting precipitate was isolated by filtration to yield the title compound as a dark green solid (217.8 mg, 73%). M_n = 42 kDa, M_w = 184 kDa, $Đ$ = 4.4. ^{1}H NMR (500 MHz, d_2-1,1,2,2-tetrachloroethane): 8.95 (br, 2H, Ar*H*), 7.73 (br, 2H, Ar*H*), 4.25 (br, 4H, $-NCH_2-$), 1.82 (br, 8H, $-CH_2-$), 1.39 (br, 68H, $-CH_2-$), 0.93 (br, 12H, $-CH_3$). Anal. Calcd for ($C_{70}H_{96}GeN_2O_4S_4$)$_n$: C, 68.33; H, 7.86; N, 2.28. Found: C, 68.37; H, 7.96; N, 2.31.

Poly-2,7(9,9-bis(tetradecyl)-9*H*-thieno[3,2-*b*]thieno-[2″,3″:4′,5′]thieno[2′3′:4,5]germolo[2,3-*d*]thiophene)-*alt*-4,7-bis(5,4-hexadecylthiophen-2-yl)benzo[1,2,5-*c*]thiadiazole (pDTTG-DTBT(C_{16})). An oven-dried microwave vial equipped with a stir bar was charged with 2,7-bis(trimethylstannyl)-9,9-bis(tetradecyl)-9*H*-thieno[3,2-*b*]thieno[2″,3″:4′,5′]thieno[2′,3′:4,5]-germolo[2,3-*d*]-thiophene (**5**) (206.2 mg, 0.1928 mmol), 4,7-bis(5-bromo-4-hexadecylthiophen-2-yl)benzo[1,2,5-*c*]thiadiazole (174.9 mg, 0.1928 mmol), tris(dibenzylideneacetone)dipalladium(0) (3.5 mg, 0.0039 mmol), and tri(*o*-tolyl)phosphine (4.7 mg, 0.0154 mmol). The vial was purged with argon before anhydrous chlorobenzene (1.0 mL) was added. The reaction mixture was purged with argon for a further 30 min and then reacted as above. After cooling the crude product was purified exactly as for pDTTG-NDI. The isolated powder was further purified by preparative GPC (chlorobenzene) and a final precipitation to yield the title compound as a dark blue solid (203.7 mg, 71%). M_n = 27 kDa, M_w = 51 kDa, $Đ$ = 1.9. ^{1}H NMR (500 MHz, d_2-1,1,2,2-tetrachloroethane): 8.07 (br, 2H, Ar*H*), 7.90 (br, 2H, Ar*H*), 7.47 (br, 2H, Ar*H*), 2.99 (br, 4H, $-CH_2-$), 1.88 (br, 4H, $-CH_2-$), 1.74 (br, 4H, $-CH_2-$), 1.49 (br, 18H, $-CH_2-$), 1.33 (br, 82H, $-CH_2-$), 0.93 (br, 12H, $-CH_3$). Anal. Calcd for ($C_{86}H_{130}GeN_2S_7$)$_n$: C, 69.37; H, 8.80; N, 1.88. Found: C, 67.79; H, 10.02; N, 1.76.

dx.doi.org/10.1021/ma5021038 | *Macromolecules* 2014, 47, 8602−8610

Scheme 1. Synthetic Route to the DTTG-TPD, DTTG-DTBT(OC_8), DTTG-NDI, and DTTG-DTBT(C_{16}) Polymers

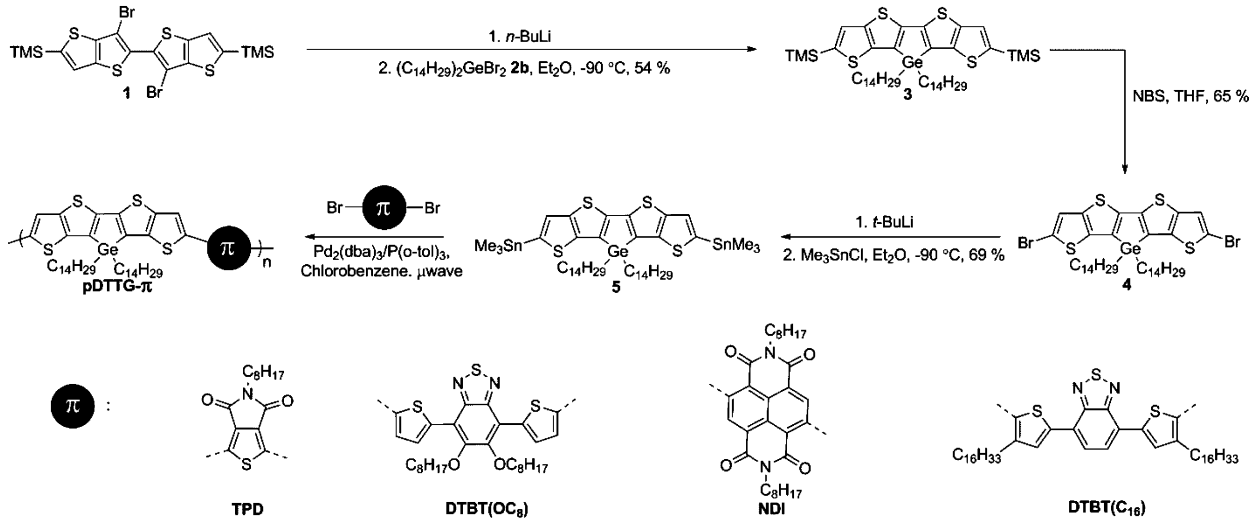

RESULTS AND DISCUSSION

Synthesis. In order to maintain a reasonable balance between solubility and synthetic availability, we chose to investigate straight chain tetradecyl side chains, for which the required Grignard reagent was commercially available. Regarding the choice of comonomer, we chose to investigate a range of electron accepting comonomer units, since the copolymerization of alternating electron donating and electron accepting units is known to be a beneficial approach towards controlling the polymer energetics and performance.[43] We initially targeted *N*-octylthienopyrrolodione (TPD) to enable a comparison to our previously reported polymer with branched side chains[35] and BT since it demonstrated good performance in the related DTG copolymers.[36] However, the absence of any solubilizing group on BT was found to result in very low polymer solubility in the present case, and we therefore focused on BT containing comonomers in which flanking thiophene groups were incorporated (DTBT). In order to improve solubility, additional side chains were incorporated either onto the flanking thiophene, as in 4,7-bis(5-bromo-4-hexadecylthiophen-2-yl)benzo[1,2,5-*c*]thiadiazole (DTBT-C_{16}) or onto the BT unit itself in 4,7-bis(5-bromothiophen-2-yl)-5,6-bis(octyloxy)benzo[1,2,5-*c*]thiadiazole (DTBT-OC_8). The structures of the comonomers are shown in Scheme 1. As a final comonomer unit, we chose *N*,*N*′-bis(*n*-octyl)-2,6-dibromonaphthalene-1,4,5,8-tetracarboxylic diimide (NDI) due to the known strong electron accepting ability of NDI's and the promising performance of NDI copolymers with fused aromatic monomers.[44,45] In particular, we were interested to observe if we could induce any electron transporting behavior in the DTTG copolymers by the inclusion of such an electron accepting comonomer.[46,47]

The synthesis of the DTTG monomer follows our previously reported methodology,[35] in which (3,3′-dibromo-2,2′-bithieno[3,2-*b*]thiene-5,5′-diyl)bis(trimethylsilane) (**1**) was dilithiated at low temperature and reacted with 1 equiv. of dibromobis(tetradecyl)germane (**2**) to afford the novel [9,9-bis(tetradecyl)-9*H*-thieno[3,2-*b*]thieno[2″,3″:4′,5′]thieno[2′,3′:4,5]germolo[2,3-*d*]thiene-2,7-diyl]bis(trimethylsilane) (**3**). Subsequent bromination with *N*-bromosuccinimide followed by lithiation with *tert*-butyllithium at −90 °C and reaction with trimethyltin chloride afforded the requisite stannylated monomer (**5**). As we previously observed, the tin monomer was prone to destannylation on normal phase silica and was instead purified by preparative GPC over cross-linked polystyrene. All four polymers, shown in Scheme 1 were synthesized via microwave assisted Stille cross-coupling reactions in chlorobenzene, using $Pd_2(dba)_3$ and P(o-Tol)$_3$ as the catalyst system.[48] After precipitation and purification by Soxhlet extraction to remove low molecular weight oligomers, the polymers were dissolved in chloroform and vigorously stirred with aqueous sodium diethyldithiocarbamate to remove residual catalytic impurities.[49] Polymers of sufficient solubility [TPD and DTBT(C_{16})] were then further purified by preparative GPC at 80 °C, using chlorobenzene as eluent. For pDTTG-DTBT(OC_8), we found that the solubility of the purified polymer was poor, even in hot 1,2-dichlorobenzene, and therefore preparative GPC was not possible. Instead, the polymer was heated in 1,1,2,2-tetrachloroethane overnight and filtered hot to remove insoluble residues.[50] Upon concentration and precipitation, a soluble fraction of pDTTG-DTBT(OC_8) was isolated. However, the majority of the yield was insoluble material.

The structure of the polymers was confirmed by a combination of elemental analysis, which were in agreement with the theoretical values and high temperature ^{1}H NMR spectroscopy, in d_2-1,1,2,2-tetrachloroethane. As is typical for many conjugated polymers, the ^{1}H spectra were rather poorly resolved due to the segmental aggregation of the polymers in solution (see Supporting Information).

Molecular weights and dispersity were determined by gel permeation chromatography in 80 °C chlorobenzene (see Supporting Information). The number-average molecular weights of pDTTG-DTBT(OC_8), pDTTG-NDI, and pDTTG-DTBT(C_{16}) were of similar magnitude as shown in Table 1. However, we note that the molecular weight of pDTTG-TPD was considerably lower. We performed three separate polymerizations for pDTTG-TPD using different batches of monomer as well as monomer concentrations, but in all cases similar molecular weights were obtained. The polymer exhibits reasonable solubility so we do not believe the low weight is caused by precipitation of the polymer during the polymerization but is rather associated with poor reactivity under the polymerization conditions.

dx.doi.org/10.1021/ma5021038 | *Macromolecules* 2014, 47, 8602−8610

Table 1. Molecular Weights and Thermal Properties of the Polymers

polymer	M_n[a] (kDa)	M_w[a] (kDa)	$Đ$[a]	T_d[b] (°C)
DTTG-TPD	7	10	1.5	432
DTTG-DTBT(OC_8)	35	88	2.5	350
DTTG-NDI	42	184	4.4	440
DTTG-DTBT(C_{16})	27	51	1.9	437

[a]Number-average molecular weights (M_n), weight-average molecular weights (M_w), and dispersity ($Đ$) determined by gel permeation chromatography (GPC) using polystyrene standards and chlorobenzene as eluent. [b]5% weight loss temperatures measured by thermal gravimetric analysis (TGA) under a nitrogen atmosphere.

Thermogravimetric analysis demonstrated that all four polymers exhibited good thermal stability, with a 5% weight loss occurring after 350 °C for pDTTG-DTBT(OC_8) and 430 °C for the remaining polymers (see Supporting Information). No obvious thermal transitions were observed by differential scanning calorimetry in the temperature range of −30 to 380 °C for any of the polymers (see Supporting Information).

Optoelectronic Properties. The optical absorption spectra of the polymers in dilute chlorobenzene and as thin films spin-cast from chlorobenzene are shown in Figure 1. This data is also summarized in Table 2. In solution, pDTTG-TPD, pDTTG-DTBT(OC_8), and pDTTG-DTBT(C_{16}) exhibit absorption maxima at 590, 595, and 605 nm, respectively. Upon film formation, these absorption maxima peaks are red-shifted to 598, 612, and 661 nm, respectively, and in the case of pDTTG-TPD, a pronounced shoulder appears at 653 nm. There is also a less well-defined shoulder in the case of pDTTG-DTBT(C_{16}) at 726 nm. The spectrum of pDTTG-TPD is very similar to that observed for the polymer with branched 2-ethylhexyl or 2-octyldodecyl groups on the DTTG unit, even though the reported molecular weight is significantly higher for both of these polymers.[34,35] This similarity suggests the effective conjugative length has been reached for pDTTG-TPD in the present case. The red-shifts observed upon film formation and the appearance of the long wavelength shoulders are indicative of backbone planarization and enhanced intermolecular ordering. Interestingly, we observe that the red-shift of pDTTG-DTBT(C_{16}) upon film formation is significantly larger than that observed for the other polymers. We believe this is related to the more torsionally twisted structure of pDTTG-DTBT(C_{16}) in solution compared to the other polymers. The regiochemistry of the hexadecyl side chains in pDTTG-DTBT(C_{16}) results in some steric interaction of the DTBT unit and the adjacent DTTG, likely causing a more twisted structure (see DFT section for more details). Solid state packing forces can overcome these perturbations, leading to a more planar backbone in the solid state.

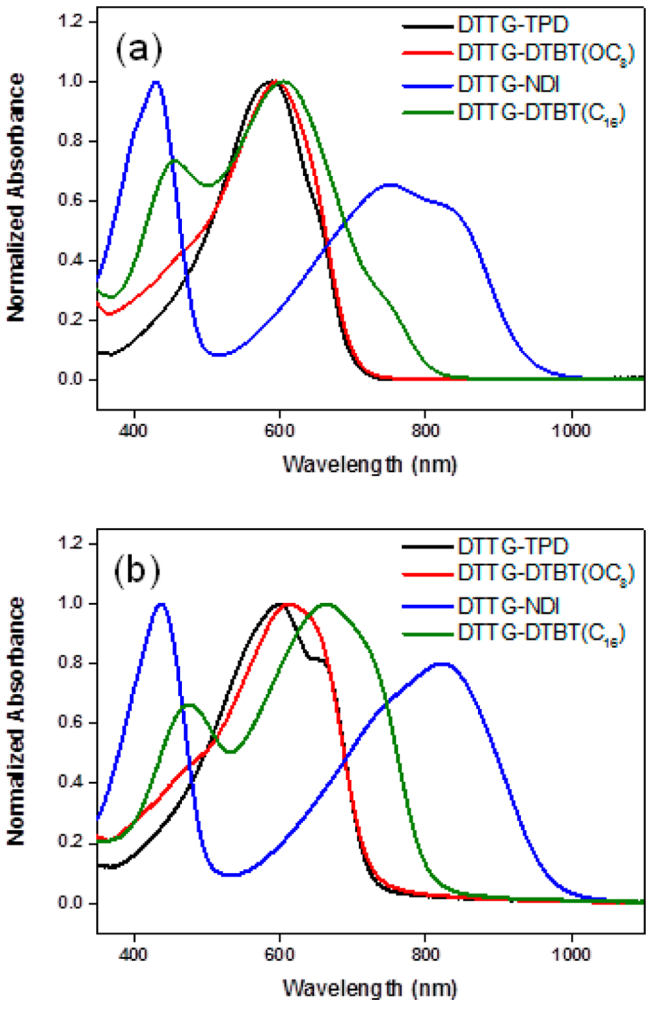

Figure 1. Normalized UV−vis absorption spectra of the polymers in (a) dilute chlorobenzene solutions and (b) thin films spin-cast from 5 mg/mL chlorobenzene solution.

The inclusion of the strong acceptor NDI leads to a significant broadening of the absorption spectra, which spans the visible to near-infrared range, with an absorption maximum at 752 nm and a pronounced shoulder at 824 nm. Upon solidification, the intensity of this shoulder increases, and it now becomes the maximum absorption peak. The spectrum also slightly broadens with a red-shift in the onset of absorption, leading to a low optical band gap of 1.36 eV.

The ionization potential of the polymers as thin films spin-cast from chlorobenzene was measured using photoelectron spectroscopy in air (PESA), and the HOMO energy was approximated as the negative of the ionization potential. This data is summarized in Table 2. The nature of the comonomer was found to have a significant impact on the ionization potential of the polymer. Thus, the inclusion of the strong electron acceptor NDI resulted in a polymer with a high ionization potential of 5.50 eV. Replacement of NDI with the less electron accepting TPD decreased the ionization potential to 5.24 eV, which is slightly lower than that previously observed for the branched 2-ethylhexyl polymer by the same technique (5.33 eV),[34] again suggesting the effective conjugation length has been reached despite the low molecular weight. The difference of 0.09 eV between the tetradecyl-substituted polymer and the 2-ethylhexyl polymer previously reported is within the error of the measurements (±0.05 eV), so it is difficult to draw any conclusions about the influence of the side chain.

For both of the DTBT polymers, the ionization potentials are substantially increased to 4.80 and 4.84 eV for pDTTG-DTBT(OC_8) and pDTTG-DTBT(C_{16}), respectively. The increase in ionization potential is likely related to the presence of the additional electron-rich thiophene flanking groups in the DTBT unit. Interestingly, the substitution pattern of the DTBT unit, either as electron donating alkoxy groups on the BT core or alkyl chains on the flanking thiophenes, does not make a

dx.doi.org/10.1021/ma5021038 | Macromolecules 2014, 47, 8602−8610

Table 2. Frontier Molecular Orbital Energy Levels and Optical Properties of the Polymers

polymer	λ_{max} soln[a] (nm)	λ_{max} film[b] (nm)	HOMO[c] (eV)	LUMO[d] (eV)	E_g opt[e] (eV)	HOMO[f] (eV)	LUMO[f] (eV)	E_g opt[f] (eV)
DTTG-TPD	590	598	−5.24	−3.53	1.71	−5.10	−3.26	1.84
DTTG-DTBT(OC_8)	595	612	−4.80	−3.09	1.71	−4.79	−3.17	1.62
DTTG-NDI	752	824	−5.50	−4.23	1.27	−5.28	−3.92	1.36
DTTG-DTBT(C_{16})	605	661	−4.84	−3.30	1.54	−4.85	−3.38	1.47

[a]Measured in dilute chlorobenzene solution at 20 °C. [b]Thin films spin-cast on glass substrates from 5 mg/mL chlorobenzene solution. [c]HOMO was approximated by taking the negative ionization potential determined by PESA (error ±0.05 eV). [d]LUMO was estimated by adding the HOMO energy level to the absorption onset in the solid state. [e]Optical band gap determined from the absorption onset in the solid state. [f]Calculated by DFT using the minimum energy conformation of the trimers at the B3LYP/6-311G(D) level. Alkyl chains were substituted for methyl groups.

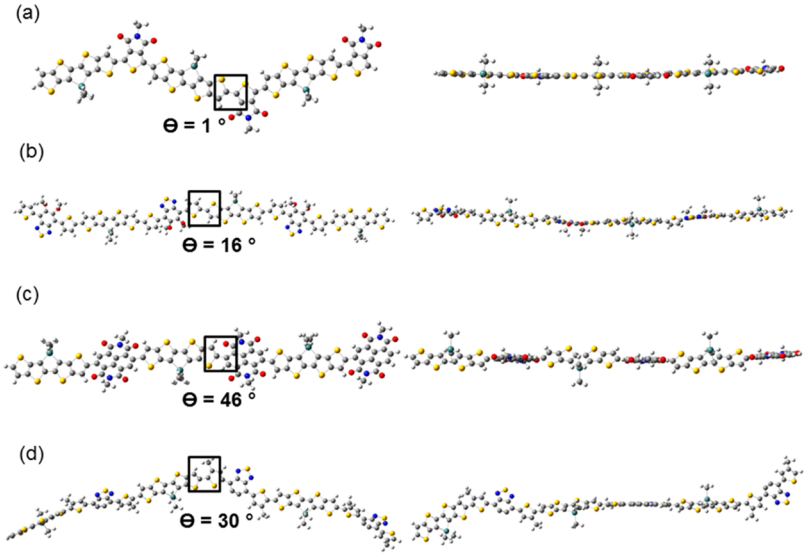

Figure 2. Face-on (left) and side-on (right) DFT images of the minimum-energy conformation of the trimers (a) pDTTG-TPD, (b) pDTTG-DTBT(OC_8), (c) pDTTG-NDI, and (d) pDTTG-DTBT(C_{16}) at the B3LYP/6-311G(D) level. The torsion angle (Θ) between the central DTTG unit and the adjacent aromatic is highlighted. Alkyl chains were substituted for methyl groups.

large difference to the ionization potential. We could not measure the LUMO level directly but have estimated the value by adding the optical band gap, as measured from the onset of absorption, to the HOMO level. Although such an estimate does not take into account the exciton binding energy, it allows for a convenient comparison between the different polymers. Here we see that the inclusion of NDI results in a substantial lowering of the LUMO to a level where electron injection from common source drain electrodes might be expected in transistor devices.

Polymer Conformation and Packing. Density functional theory (DFT) was also used to evaluate the frontier molecular orbital energy levels and optimized geometry of all four polymers in vacuum. Calculations were carried out at the B3LYP[51] hybrid functional level of theory using a 6-311G(D) basis set. Each polymer was modeled as a trimer, with alkyl chains substituted for methyl groups in order to reduce the computational cost. As shown in Table 2, the trends observed in the computationally calculated HOMO and LUMO energy level values are in good agreement with those observed experimentally. Differences in the absolute values can be attributed to the inherent limitations of the DFT model to accurately describe organic semiconducting polymers.[52] Visualization of the calculated HOMO and LUMO energy level electron density plots can be found in the Supporting Information. For all polymers except pDTTG-NDI, the HOMO is delocalized over the whole backbone, whereas the NDI copolymer shows a localization of the wave function on the DTTG unit. In contrast, the LUMO is effectively delocalized over the backbone for pDTTG-NDI and pDTTG-TPD, but for both polymers containing the BT unit, the LUMO is relatively localized over the BT unit.

The minimum-energy conformation of all four polymers calculated using DFT is shown in Figure 2. In order to minimize the possibility of obtaining a local energy minima, calculations were performed for each polymer starting from a variety of conformations with respect to the DTTG and the comonomers, and these were allowed to relax to an energy minimum. Frequency calculations were then performed on these lowest energy conformers to ensure the geometry was not the result of a local minimum. In order to minimize the number of calculations, the relative geometry of the DTBT unit was always considered from a starting point of one thiophene facing the N of the thiadiazole ring and one facing the opposite direction. The relative conformation of the DTBT unit relative to the DTTG (i.e., syn or anti with respect to the thiophene) was then varied. The lowest energy conformers found are shown in Figure 2.

The main conclusion of these calculations is that there are substantial differences in the backbone planarity for the polymers, in particular for pDTTG-DTBT(C_{16}) and pDTTG-DTBT(OC_8) which are structurally similar. In the case of the latter, inclusion of the alkoxy groups on the BT unit only results in a small torsional twist with the flanking thiophene, in agreement with previous calculations,[53] and there is also only a small twist between the DTTG and the thiophene (Θ = 16°).

dx.doi.org/10.1021/ma5021038 | Macromolecules 2014, 47, 8602−8610

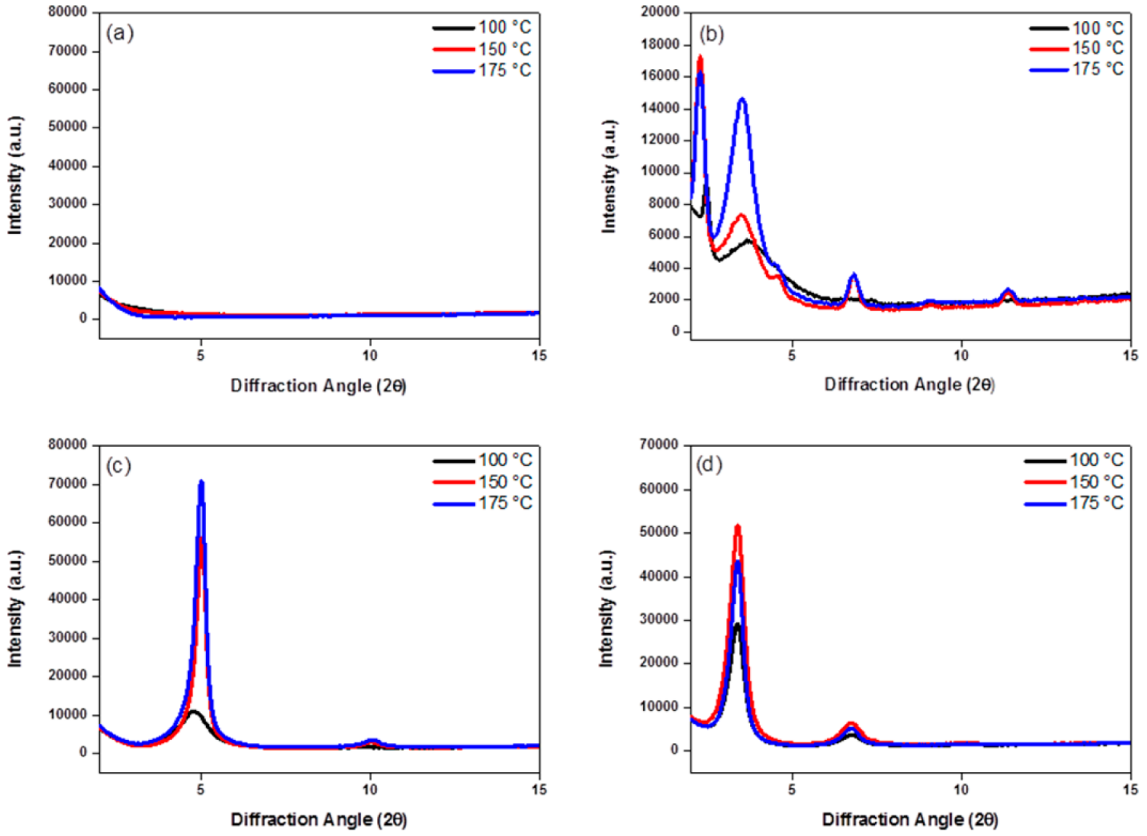

Figure 3. X-ray diffraction patterns of (a) pDTTG-TPD, (b) pDTTG-DTBT(OC_8), (c) pDTTG-NDI, and (d) pDTTG-DTBT(C_{16}) drop-cast from 7 mg/mL 1,2-dichlorobenzene solution on glass substrates and thermally annealed at 100 °C (black line), 150 °C (red line), and 175 °C (blue line) for 2 min under an argon atmosphere.

In contrast for pDTTG-DTBT(C_{16}) although the thiophene-BT unit only has a small twist, the torsional twist between the DTTG and thiophene is larger ($\Theta = 30°$), as a result of steric interactions between the alkyl side-chain and the DTTG. The net result is a much contorted backbone. The structure of pDTTG-NDI also predicts a relatively large torsional twist between the DTTG and the NDI unit ($\Theta = 46°$), in agreement with other calculations on fused thiophene NDI copolymers.[46] Finally, in the case of the TPD copolymer, a fully coplanar backbone is predicted.

The thin film morphology of the polymers was studied using out-of-plane X-ray diffraction measurements. The diffraction patterns of all four polymers, drop-cast from 1,2-dichlorobenzene and annealed at 100, 150, or 175 °C for 2 min, are shown in Figure 3. No diffraction peaks were observed for pDTTG-TPD at any of the temperatures studied, in contrast to the fact that the analogous polymer with 2-ethylhexyl side chains showed diffraction peaks associated with lamellar ordering.[35] However, since the polymer with longer 2-octyldodecyl side chains also showed much weaker diffraction,[34] we believe the presence of long side chains, such as tetradecyl in the present example, disrupts any lamellar type ordering. All of the other three polymers appear more ordered than pDTTG-TPD. pDTTG-DTBT(OC_8), pDTTG-NDI, and pDTTG-DTBT-(C_{16}) all exhibit a first-order diffraction peak at $2\Theta = 3.6°$, 4.8°, and 3.4°, corresponding to a *d*-spacing of 24.2, 18.4, and 26.1 Å, respectively, after annealing at 100 °C. For pDTTG-DTBT(C_{16}) a weak second-order diffraction peak at $2\Theta = 6.8°$ is also observed after annealing at 100 °C. Annealing at higher temperatures (150 or 175 °C) results in a slight decrease of the *d*-spacing for pDTTG-DTBT(C_{16}) to 25.2 Å but little change in the intensity of the diffraction peaks. For pDTTG-DTBT(OC_8) and pDTTG-NDI annealing at 150 and 175 °C results in a significant increase in intensity of the main diffraction peak, and the appearance of second-order diffraction peaks at $2\Theta = 6.8°$ and 10.0° for pDTTG-DTBT(OC_8) and pDTTG-NDI, respectively. For pDTTG-DTBT(OC_8) a third-order diffraction peak observed at $2\Theta = 11.4°$ is also observed. For both of these polymers, despite the absence of any transitions on the DSC trace, it is clear that annealing at 150 °C or above results in an increase in thin film order. Full XRD plots at larger diffraction angles (2Θ up to 30°) are shown in Figure S13, but only weak and very broad diffraction peaks are observed at longer wavelengths, which are likely related to slight variations in the scatter from the glass slide background.

Transistor Devices. In order to investigate the charge transport behavior of the polymers, top gate, bottom contact OFET devices were fabricated using Lisicon D139, a fluoropolymer, as the dielectric and silver source drain electrodes. Polymer films were spin-cast from 1,2-dichlorobenzene solutions and annealed at 100 °C for 2 min for initial testing. pDTTG-TPD, pDTTG-DTBT(C_{16}), and pDTTG-DTBT(OC_8) all exhibited p-type behavior with average saturated mobilities around 0.02 $cm^2\ V^{-1}\ s^{-1}$ for the TPD and DTBT(C_{16}) polymers and a lower value of 0.002 $cm^2\ V^{-1}\ s^{-1}$ for the DTBT(OC_8) polymer (see Supporting Information). In agreement with the low-lying LUMO of pDTTG-NDI, we observe ambipolar behavior, with average saturated hole and electron mobilities of 0.0007 and 0.003 $cm^2\ V^{-1}\ s^{-1}$, respectively. Annealing the films to a higher temperature (150

dx.doi.org/10.1021/ma5021038 | *Macromolecules* 2014, 47, 8602−8610

or 175 °C) had little effect on the performance of pDTTG-TPD, in agreement with the lack of changes observed by XRD. A modest improvement of the mobility by a factor of 2 was observed for pDTTG-DTBT(OC_8) upon annealing at either 150 or 175 °C. Better performance was observed for pDTTG-DTBT(C_{16}) upon annealing, which exhibits a promising peak mobility of 0.056 $cm^2\ V^{-1}\ s^{-1}$ in the linear regime upon annealing at 150 °C.

The promising performance of pDTTG-DTBT(C_{16}) prompted us to investigate its performance more closely. One of the drawbacks of many conjugated polymers is the fact that they are only soluble in halogenated solvents, like chloroform or 1,2-dichlorobenzene. The use of such solvents is problematic in industrial processes because of their health hazards and detrimental environmental impact.[54] Therefore, the development of conjugated polymers which can be processed from non-chlorinated solvents without any reduction in device performance is of particular interest. Gratifyingly, we find that in the present case pDTTG-DTBT(C_{16}) is soluble in a 1:1 mixture of 1,3,5-trimethylbenzene:1-methylnaphthalene at a concentration of 7 mg/mL. The presence of the long side chains on the DTBT unit and the torsional twist of the polymer in solution help to ensure good solubility. This solvent mixture was developed because of the similarity in boiling point and Hansen dispersive solubility parameters[55] to dichlorobenzene. A solvent mixture with a high boiling point was desirable to allow the polymer time to organize during the coating of the film. The transistor performance of devices coated from this mixed solvent and annealed for 2 min at 150 °C was considerably higher than that of the devices coated from 1,2-dichlorobenzene (Figure 4). The devices displayed saturated and linear peak mobilities of 0.22 and 0.26 $cm^2\ V^{-1}\ s^{-1}$, respectively, without strong gate voltage dependence. To the best of our knowledge, this is the highest reported charge carrier mobility of any germanium-based polymer reported to date and demonstrates the DTTG motif has potential as a building block in the development of conjugated polymers for transistor applications.

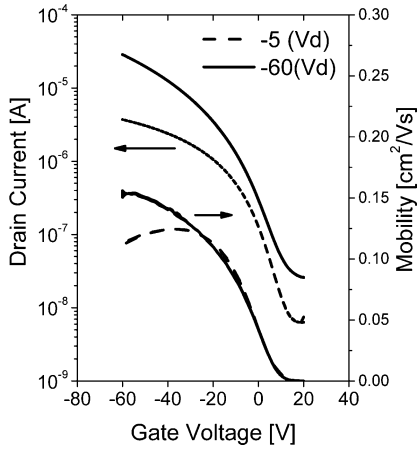

Figure 4. Typical transfer characteristics and gate voltage dependence of mobility of top gate, bottom contact pDTTG-DTBT(C_{16}) devices with Ag source/drain electrodes processed from 1,3,5-trimethylbenzene:1-methylnaphthalene (1:1, 7 mg/mL) annealed at 150 °C (channel length L = 20 μm, channel width W = 1000 μm).

CONCLUSION

In this work we report the synthesis of the first dithienogemolodithiophene monomers containing straight chain tetradecyl groups. We report the copolymerization of this monomer with four different acceptor units and show how the choice of acceptor influences the optical properties and molecular energy levels. All four polymer exhibit similar thermal properties in TGA and DSC measurements but display significant differences in solid state packing as observed by XRD. Computational modeling of oligomers by DFT gives some insight into the different backbone conformations of the different polymers. Field effect transistor devices were also fabricated and one copolymer displays encouraging transistor performance. Importantly, this copolymer is soluble in non-chlorinated solvents, and using a mixture of aromatic solvents, we were able to fabricate transistor devices with field-effect mobility up to 0.26 $cm^2\ V^{-1}\ s^{-1}$. These results suggest DTTG is a useful building block for the development of high performance semiconducting polymers.

ASSOCIATED CONTENT

Supporting Information

^{1}H NMR of the distannylated monomer (**5**), ^{1}H NMR of all four polymers, polymer GPC chromatographs, polymer DSC plots, polymer TGA traces, and OFET device characteristics. This material is available free of charge via the Internet at http://pubs.acs.org.

AUTHOR INFORMATION

Corresponding Author

*E-mail m.heeney@imperial.ac.uk (M.H.).

Present Address

H.Z.: Department of Materials Science and Engineering, University of Washington, Seattle, WA 98195-2120.

Notes

The authors declare no competing financial interest.

ACKNOWLEDGMENTS

We thank Merck Chemicals for the financial support of an EPSRC iCASE award and for their input and support of this project. We gratefully acknowledge Dr. Scott E Watkins (CSIRO) for the PESA measurements.

REFERENCES

(1) Sirringhaus, H. *Adv. Mater.* **2014**, *26*, 1319−1335.
(2) Dong, H.; Fu, X.; Liu, J.; Wang, Z.; Hu, W. *Adv. Mater.* **2013**, *25*, 6158−6183.
(3) Holliday, S.; Donaghey, J. E.; McCulloch, I. *Chem. Mater.* **2014**, *26*, 647−663.
(4) Zhao, Y.; Guo, Y.; Liu, Y. *Adv. Mater.* **2013**, *25*, 5372−5391.
(5) Biniek, L.; Schroeder, B. C.; Nielsen, C. B.; McCulloch, I. *J. Mater. Chem.* **2012**, *22*, 14803−14813.
(6) Wang, C.; Dong, H.; Hu, W.; Liu, Y.; Zhu, D. *Chem. Rev.* **2012**, *112*, 2208−2267.
(7) Tsao, H. N.; Cho, D. M.; Park, I.; Hansen, M. R.; Mavrinskiy, A.; Yoon, D. Y.; Graf, R.; Pisula, W.; Spiess, H. W.; Müllen, K. *J. Am. Chem. Soc.* **2011**, *133*, 2605−2612.
(8) Li, Y.; Singh, S. P.; Sonar, P. *Adv. Mater.* **2010**, *22*, 4862−4866.
(9) Wang, S.; Kappl, M.; Liebewirth, I.; Müller, M.; Kirchhoff, K.; Pisula, W.; Müllen, K. *Adv. Mater.* **2012**, *24*, 417−420.
(10) Li, Y.; Sonar, P.; Singh, S. P.; Soh, M. S.; van Meurs, M.; Tan, J. *J. Am. Chem. Soc.* **2011**, *133*, 2198−2204.

(11) Shahid, M.; McCarthy-Ward, T.; Labram, J.; Rossbauer, S.; Domingo, E. B.; Watkins, S. E.; Stingelin, N.; Anthopoulos, T. D.; Heeney, M. *Chem. Sci.* **2012**, *3*, 181−185.
(12) Tseng, H.-R.; Phan, H.; Luo, C.; Wang, M.; Perez, L. A.; Patel, S. N.; Ying, L.; Kramer, E. J.; Nguyen, T.-Q.; Bazan, G. C.; Heeger, A. J. *Adv. Mater.* **2014**, *26*, 2993−2998.
(13) Chen, H.; Guo, Y.; Mao, Z.; Yu, G.; Huang, J.; Zhao, Y.; Liu, Y. *Chem. Mater.* **2013**, *25*, 3589−3596.
(14) Chen, H.; Guo, Y.; Yu, G.; Zhao, Y.; Zhang, J.; Gao, D.; Liu, H.; Liu, Y. *Adv. Mater.* **2012**, *24*, 4618−4622.
(15) Kang, I.; An, T. K.; Hong, J.; Yun, H.-J.; Kim, R.; Chung, D. S.; Park, C. E.; Kim, Y.-H.; Kwon, S.-K. *Adv. Mater.* **2013**, *25*, 524−528.
(16) Kim, G.; Kang, S.-J.; Dutta, G. K.; Han, Y.-K.; Shin, T. J.; Noh, Y.-Y.; Yang, C. *J. Am. Chem. Soc.* **2014**, *136*, 9477−9483.
(17) Shin, J.; Um, H. A.; Lee, D. H.; Lee, T. W.; Cho, M. J.; Choi, D. H. *Polym. Chem.* **2013**, *4*, 5688−5695.
(18) Yuen, J. D.; Fan, J.; Seifter, J.; Lim, B.; Hufschmid, R.; Heeger, A. J.; Wudl, F. *J. Am. Chem. Soc.* **2011**, *133*, 20799−20807.
(19) Sun, B.; Hong, W.; Yan, Z.; Aziz, H.; Li, Y. *Adv. Mater.* **2014**, *26*, 2636−2642.
(20) Li, J.; Zhao, Y.; Tan, H. S.; Guo, Y.; Di, C.-A.; Yu, G.; Liu, Y.; Lin, M.; Lim, S. H.; Zhou, Y.; Su, H.; Ong, B. S. *Sci. Rep.* **2012**, *2*, 754.
(21) Bronstein, H.; Chen, Z.; Ashraf, R. S.; Zhang, W.; Du, J.; Durrant, J. R.; Tuladhar, P. S.; Song, K.; Watkins, S. E.; Geerts, Y.; Wienk, M. M.; Janssen, R. a J.; Anthopoulos, T.; Sirringhaus, H.; Heeney, M.; McCulloch, I. *J. Am. Chem. Soc.* **2011**, *133*, 3272−3275.
(22) Yan, H.; Chen, Z.; Zheng, Y.; Newman, C.; Quinn, J. R.; Dötz, F.; Kastler, M.; Facchetti, A. *Nature* **2009**, *457*, 679−686.
(23) Kang, I.; Yun, H.-J.; Chung, D. S.; Kwon, S.-K.; Kim, Y.-H. *J. Am. Chem. Soc.* **2013**, *135*, 14896−14899.
(24) Xu, Y.-X.; Chueh, C.-C.; Yip, H.-L.; Ding, F.-Z.; Li, Y.-X.; Li, C.-Z.; Li, X.; Chen, W.-C.; Jen, A. K.-Y. *Adv. Mater.* **2012**, *24*, 6356−6361.
(25) Li, Y.; Yao, K.; Yip, H.-L.; Ding, F.-Z.; Xu, Y.-X.; Li, X.; Chen, Y.; Jen, A. K.-Y. *Adv. Funct. Mater.* **2014**, *24*, 3631−3638.
(26) Ashraf, R. S.; Chen, Z.; Leem, D. S.; Bronstein, H.; Zhang, W.; Schroeder, B.; Geerts, Y.; Smith, J.; Watkins, S.; Anthopoulos, T. D.; Sirringhaus, H.; de Mello, J. C.; Heeney, M.; McCulloch, I. *Chem. Mater.* **2011**, *23*, 768−770.
(27) Zhang, W.; Smith, J.; Watkins, S. E.; Gysel, R.; McGehee, M.; Salleo, A.; Kirkpatrick, J.; Ashraf, S.; Anthopoulos, T.; Heeney, M.; McCulloch, I. *J. Am. Chem. Soc.* **2010**, *132*, 11437−11439.
(28) Bronstein, H.; Leem, D. S.; Hamilton, R.; Woebkenberg, P.; King, S.; Zhang, W.; Ashraf, R. S.; Heeney, M.; Anthopoulos, T. D.; Mello, J.; De McCulloch, I. *Macromolecules* **2011**, *44*, 6649−6652.
(29) Mei, J.; Bao, Z. *Chem. Mater.* **2014**, *26*, 604−615.
(30) Lei, T.; Wang, J.-Y.; Pei, J. *Chem. Mater.* **2014**, *26*, 594−603.
(31) Dou, J.-H.; Zheng, Y.-Q.; Lei, T.; Zhang, S.-D.; Wang, Z.; Zhang, W.-B.; Wang, J.-Y.; Pei, J. *Adv. Funct. Mater.* **2014**, DOI: 10.1002/adfm.201401822.
(32) Meager, I.; Ashraf, R. S.; Mollinger, S.; Schroeder, B. C.; Bronstein, H.; Beatrup, D.; Vezie, M. S.; Kirchartz, T.; Salleo, A.; Nelson, J.; McCulloch, I. *J. Am. Chem. Soc.* **2013**, *135*, 11537−11540.
(33) Lei, T.; Dou, J.-H.; Pei, J. *Adv. Mater.* **2012**, *24*, 6457−6461.
(34) Zhong, H.; Li, Z.; Buchaca-Domingo, E.; Rossbauer, S.; Watkins, S. E.; Stingelin, N.; Anthopoulos, T. D.; Heeney, M. *J. Mater. Chem. A* **2013**, *1*, 14973−14981.
(35) Zhong, H.; Li, Z.; Deledalle, F.; Fregoso, E. C.; Shahid, M.; Fei, Z.; Nielsen, C.; Yaacobi-Gross, N.; Rossbauer, S.; Anthopoulos, T. D.; Durrant, J. R.; Heeney, M. *J. Am. Chem. Soc.* **2013**, *135*, 2040−2043.
(36) Fei, Z.; Kim, J. S.; Smith, J.; Domingo, E. B.; Anthopoulos, T. D.; Stingelin, N.; Watkins, S. E.; Kim, J.-S.; Heeney, M. *J. Mater. Chem.* **2011**, *21*, 16257−16263.
(37) Frisch, M. J.; Trucks, G. W.; Schlegel, H. B.; Scuseria, G. E.; Robb, M. A.; Cheeseman, J. R.; Montgomery, Jr., J. A.; Vreven, T.; Kudin, K. N.; Burant, J. C.; Millam, J. M.; Iyengar, S. S.; Tomasi, J.; Barone, V.; Mennucci, B.; Cossi, M.; Scalmani, G.; Rega, N.; et al. Gaussian 03, Revision E.01, 2004.
(38) Frisch, M. J.; Trucks, G. W.; Schlegel, H. B.; Scuseria, G. E.; Robb, M. A.; Cheeseman, J. R.; Scalmani, G.; Barone, V.; Mennucci, B.; Petersson, G. A.; Nakatsuji, H.; Caricato, M.; Li, X.; Hratchian, H. P.; Izmaylov, A. F.; Bloino, J.; Zheng, G.; Sonnenb, D. J.; et al. Gaussian 09, Revision C.01, 2009.
(39) Cabanetos, C.; Labban, A. El; Bartelt, J. A.; Douglas, J. D.; Mateker, W. R.; Frechet, J. M. J.; Mcgehee, M. D.; Beaujuge, P. M. *J. Am. Chem. Soc.* **2013**, *135*, 4656−4659.
(40) Chen, Z.; Zheng, Y.; Yan, H.; Facchetti, A. *J. Am. Chem. Soc.* **2009**, *131*, 8−9.
(41) Mishra, S. P.; Palai, A. K.; Srivastava, R. *J. Polym. Sci., Part A: Polym. Chem.* **2009**, *47*, 6514−6525.
(42) Qin, R.; Li, W.; Li, C.; Du, C.; Veit, C.; Schleiermacher, H.-F.; Andersson, M.; Bo, Z.; Liu, Z.; Inganäs, O.; Wuerfel, U.; Zhang, F. *J. Am. Chem. Soc.* **2009**, *131*, 14612−14613.
(43) Guo, X.; Baumgarten, M.; Müllen, K. *Prog. Polym. Sci.* **2013**, *38*, 1832−1908.
(44) Yuan, M.; Durban, M. M.; Kazarinoff, P. D.; Zeigler, D. F.; Rice, A. H.; Segawa, Y.; Luscombe, C. K. *J. Polym. Sci., Part A: Polym. Chem.* **2013**, *51*, 4061−4069.
(45) Guo, X.; Kim, F. S.; Seger, M. J.; Jenekhe, S. A.; Watson, M. D. *Chem. Mater.* **2012**, *24*, 1434−1442.
(46) Luzio, A.; Fazzi, D.; Natali, D.; Giussani, E.; Baeg, K.-J.; Chen, Z.; Noh, Y.-Y.; Facchetti, A.; Caironi, M. *Adv. Funct. Mater.* **2014**, *24*, 1151−1162.
(47) Guo, X.; Facchetti, A.; Marks, T. J. *Chem. Rev.* **2014**, *114*, 8943−9021.
(48) Tierney, S.; Heeney, M.; McCulloch, I. *Synth. Met.* **2005**, *148*, 195−198.
(49) Krebs, F. C.; Nyberg, B.; Jørgensen, M.; Energy, A. B. S.; Sol, M. *Chem. Mater.* **2004**, *16*, 1313−1318.
(50) Hendriks, K. H.; Heintges, G. H. L.; Gevaerts, V. S.; Wienk, M. M.; Janssen, R. A. J. *Angew. Chem., Int. Ed.* **2013**, *52*, 8341−8344.
(51) Becke, A. D. *J. Chem. Phys.* **1993**, *98*, 5648.
(52) Risko, C.; McGehee, M. D.; Brédas, J.-L. *Chem. Sci.* **2011**, *2*, 1200−1218.
(53) Casey, A.; Ashraf, R. S.; Fei, Z.; Heeney, M. *Macromolecules* **2014**, *47*, 2279−2288.
(54) Lee, W.-Y.; Giri, G.; Diao, Y.; Tassone, C. J.; Matthews, J. R.; Sorensen, M. L.; Mannsfeld, S. C. B.; Chen, W.-C.; Fong, H. H.; Tok, J. B.-H.; Toney, M. F.; He, M.; Bao, Z. *Adv. Funct. Mater.* **2014**, *24*, 3524−3534.
(55) Hansen, C. M. *Hansen Solubility Parameters: A User's Handbook*, 2nd ed.; CRC Press: Boca Raton, FL, 2007.